Ultrathin Diamond-like Carbon Film Coated Silver Nanoparticles-Based Substrates for Surface-Enhanced Raman Spectroscopy

Fanxin Liu,* Zhishen Cao, Chaojun Tang, Ling Chen, and Zhenlin Wang*

National Laboratory of Solid State Microstructures and Department of Physics, Nanjing University, Nanjing 210093, P R China

ABSTRACT We have demonstrated that by coating with a thin dielectric layer of tetrahedral amorphous carbon (ta-C), a biocompatible and optical transparent material in the visible range, the Ag nanoparticle-based substrate becomes extremely suitable for surface-enhanced Raman spectroscopy (SERS). Our measurements show that a 10 Å or thicker ta-C layer becomes efficient to protect the oxygen-free Ag in air and prevent Ag ionizing in aqueous solutions. Furthermore, the Ag nanoparticles substrate coated with a 10 Å ta-C film shows a higher enhancement of Raman signals than the uncoated substrate. These observations are further supported by our numerical simulations. We suggest that biomolecule detections in analytic assays could be easily realized using ta-C-coated Ag-based substrate for SERS especially in the visible range. The coated substrate also has higher mechanical stability, chemical inertness, and technological compliance, and may be useful, for example, to enhance TiO_2 photocatalysis and solar-cell efficiency by the surface plasmons.

KEYWORDS: SERS · ultrathin ta-C film · dielectric layer · Ag nanoparticles · oxygen-free

Since the discovery of the enhanced Raman signals on a roughed metallic surface, the SERS technique has been implemented widely by a broad scientific research community for chemical and biological sensing and measurements. This technique combines the capability of molecular fingerprinting with ultrahigh, even single-molecular sensitivity,[1−5] which cannot be achieved with other spectroscopic techniques. The principle of the method exploits mainly the enhancement of Raman scattering from the molecules in the proximity of nanoscale rough metal surfaces due to the coupling of an oscillating electric field of the incident and scattered radiation with surface plasmons of the metal.[6]

A convenient way to build a SERS-active substrate is to use Ag or Au nanoparticles,[7,8] either in a solution or immobilized at a dielectric surface.[9,10] Ag is generally preferred over Au as a SERS active element because of its up to 2 orders of magnitude greater enhancement factor especially in the visible spectrum region.[11] However, using Ag as a substrate is also associated with serious drawbacks for, specifically, chemical stability and biological applications. First, Ag is prone to oxidation in air or water, which will decrease its SERS activity and chemical stability.[11] Second, Ag is less biocompatible than Au, when in contact with aqueous solutions, which inevitably forms Ag^+ cations that can attack or degrade biopolymers.[6] For this reason, considerable efforts have been made to combine the better biocompatibility of Au with Ag to design Au−Ag hybrid systems, such as mixed Ag (core)/Au (shell) nanoparticles[12−14] and Ag (Au) nanoparticles.[15] Although the Ag−Au interactions allowed for a tunability of the surface plasmon resonances of the hybrid systems, none of these systems reported so far has led to optical performances comparable to that of an Ag surface. Recently an Au−Ag hybrid device was developed in which Au/Ag was separated by an ultrathin insulating organic film using an electrochemical method.[6] This device was found to exhibit an enhancement nearly the same as that of the Ag surface. The mechanism can be attributed to an efficient transfer of plasmon resonance excitation from Ag to Au. However, due to large absorption of Au in the visible, this method is efficient only in the excitation below 500 nm.[6]

In this letter, we report the observation of SERS using a diamond-like carbon (DLC) film as an ultrathin layer coated on Ag nanoparticle-based substrates. DLC film is an amorphous carbon material which contains a mixture of sp^3-bonded (as in diamond) and sp^2-bonded (as in graphite) carbon atoms.[16] Numerous types of DLC film such as hydrogenated amorphous carbon (a-C:H), tetrahedral amorphous carbon

*Address correspondence to lfx63@163.com, zlwang@nju.edu.cn.

Received for review January 10, 2010 and accepted April 26, 2010.

Published online April 30, 2010. 10.1021/nn100053s

(ta-C) *etc*., can be deposited using a variety of plasma deposition technologies.[17] But only ta-C film with sp^3 bonding up to 90% and a thickness up to 1−2 nm can preserve its extraordinary mechanical properties, thus serving as a protective coating layer.[17−19] The ta-C film as an ultrathin film has many desirable properties, such as pinhole free, chemical inertness, thermal stability, biocompatibility, high electrical resistance, and optical transparency in the visible and infrared, *etc*.[17] Compared with a polycrystalline diamond,[17,18] a ta-C film also has a distinct advantage in that it can be deposited at room temperature, thus allowing it to be deposited on a variety of substrates, from low-temperature plastics to high-temperature alloys. Another advantage is that ta-C film is atomically smooth and generally takes on the roughness of the substrate on which it is deposited, which is highly desirable for many optical and biomedical applications.[20−23]

We will show that by direct surface modification with the ultrathin ta-C films, the Ag surface becomes extremely useful as a substrate in SERS. Here, the introduction of a ultrathin ta-C layer can provide following merits for applications: (1) the ta-C films can fulfill special requirements, for example, biocompatibility; (2) ultrathin coating thickness can maintain and tune plasmon resonance excitations for Ag nanoparticles and provide a higher enhanced electric field than the uncoated substrate; and (3) this layer can also avoid the energy dissipation of an absorbed analyte molecule to metal caused by the electron−hole pair effect, hence the yield of the Raman emission can be increased.[24] The coated substrate also has higher mechanical stability, chemical inertness, and technological compliance, and may be useful, for example, for fluorophore enhancement,[25] the spaser,[26] and as TiO_2 photocatalyst.[27]

RESULTS AND DISCUSSION

In our experiment, the Ag-based substrates were fabricated using nanosphere lithography as described previously.[28−30] Then these substrates were coated with an ultrathin ta-C film with the thickness varying from 5 to 40 Å. The refractive index of ta-C films was measured to be ∼2.3 in the spectrum range from 400 to 1000 nm. In addition, the refractive index of ta-C films almost had no change from 5 to 40 Å. A water contacted angle (WCA) of ∼68° of the ta-C film is measured, which shows that the prepared ta-C films are hydrophilic. After films deposition, the roughness has a ∼0.5 Å increase due to ion beam sputtering for cleaning before coating (data not shown here). Figure 1A shows the morphology of the Ag nanoparticles substrate coated with a 10 Å ta-C film. Measurements show that the width of the nanoparticle along the perpendicular bisector is ∼100 nm and the height is ∼30 nm. In addition, the prepared Ag nanoparticle arrays show no observable deformation after coating due to low-temperature plasma deposition. Figure 1B shows transmittance spectra for Ag nanoparticle substrates coated with the ta-C films having a thickness varying from 0 to 20 Å under normal incidence of an unpolarized light. For these uniform Ag nanoparticles, the transmittance shows a broad band centered at *ca*. 520 nm which is due to a dipole resonance of the Ag nanoparticles.[29,30] This localized surface plasmon (LSP) resonance leads to a locally enhanced electromagnetic field which is responsible for the SERS presented later.[31] After ta-C films coating, the shift of the LSP resonance is very small as compared with the peak width due to an ultrathin coating thickness, though the ta-C has a high refractive index value.[3233]

The SERS spectra of the Rhodamine 6G (R6G) molecules adsorbed on the Ag nanoparticle substrates coated with different thicknesses of ta-C layer are shown in Figure 2A in which numerous peaks can be distinctly observed in the spectra. The most pronounced peaks at 1312, 1365, 1510, and 1650 cm^{-1} can be assigned to the aromatic stretching vibrations, while the peak at 610 cm^{-1} is due to the in-plane deformation vibration of a C−C−C ring.[34] Figure 2A also shows that the Raman signal intensity decreases when the ta-C thickness is increased. When the ta-C film thickness is further increased over 20 Å, the signal intensity will become weaker than that on an uncoated substrate. To compare the surface Raman enhancement on these substrates, an absolute enhancement factor (EF) can be calculated based on a simplified formula[31]

$$EF = (I_{surf}N_{vol})/(I_{vol}N_{surf})$$

where I_{vol} and I_{surf} are the conventional Raman and SERS intensities, N_{vol} and N_{surf} represent the number of molecules probed in a bulk sample and on the SERS substrate, respectively. In the calculation, only an average enhancement including the blank area of the substrates was considered, and the 1650 cm^{-1} band having the highest peak intensity was selected for such a comparison. The EF as a function of the ta-C film thickness is plotted in Figure 2B, which shows that the EF achieved by using the substrate coated with a 10 Å ta-C layer is nearly twice that on the uncoated substrate.

The above results clearly show that the EF of SERS using coated substrates decreases when the ta-C film thickness is increased beyond 5 Å. Thus, a ta-C coating layer with a thickness less than 5 Å may be preferred for the Ag-based substrate for SERS if only the enhancement effect is taken into account. On the other hand, biomolecule assays in SERS are required to maintain chemical stability and biocompatibility for Ag-based substrates. For this purpose, the thickness of the ta-C film on a Ag-based substrate needs to make a compromise to protect the oxygen-free Ag. Using ultra-high-vacuum surface analysis techniques, the evolution for the ta-C film coverage with different thicknesses on the Ag surface is shown in Figure 3. Figure 3A and Figure

3B show the depth profile monitoring of the elements of Ag, O, and C by Auger electron spectroscopy (AES). The results show that oxygen almost disappears when the thickness of the ta-C film is increased to 10 Å, whereas oxygen displays a maximum when the thickness of the ta-C film is 5 Å. This means that a ta-C film with a thickness 10 Å can efficiently protect the oxygen-free Ag. Figure 3C and Figure 3D display the Ag $3d_{5/2}$ fine spectra of the Ag-based substrates with the dielectric layer of ta-C film thickness of 5 and 10 Å by X-ray photoelectron spectroscopy (XPS). When the ta-C film is 5 Å, Ag $3d_{5/2}$ fine spectrum shows three bonding energies. The bonding energy at 369.7, 368.6, and 368.2 eV can be assigned to Ag═O, Ag−O, and Ag(0) bondings, respectively. Moreover, the Ag═O and Ag−O bondings dominate the peak of Ag $3d_{5/2}$, which means that Ag on the substrate with 5 Å ta-C coating mainly exists with a oxidation state. When the ta-C coating thickness was increased to 10 Å, however, only Ag(0) bonding exists on the Ag-based substrates (see Figure 3D). On the basisof both the AES and XPS results, a conclusion can be made that a 10 Å ta-C layer is thick enough to protect the oxygen-free Ag.[19]

According to the above discussion, as a protective layer, a 10 Å or thicker ta-C dielectric layer is efficient to protect oxygen-free Ag in air. By considering that an increase in the dielectric layer thickness will decrease the enhancement effect, a ta-C layer with the optimized thickness of 10 Å is the best for Ag-based substrate for SERS. The 10 Å ta-C-coated Ag-based substrate also shows a higher enhancement of Raman signals than does the uncoated substrate. To explore the origin of this unexpected enhancement, different possibilities are considered. First, an R6G molecule is selected because of its good adsorbability onto the silver surface.[35] In addition, the ta-C film is hydrophilic which is chemically compatible to an R6G aqueous solution, so that an R6G molecule is easily absorbed onto a coated substrate. A long incubation time and rinse process ensure that the near-saturation coverage of the adsorbed molecule single layer on the Ag surface is almost the same as that on the ta-C surface. Thus, a difference in the number of probed molecules between coated and uncoated substrates in the Raman testing can be ruled out. Second, the LSP position is nearly unchanged as compared with its relatively wide band after coating an ultrathin ta-C layer. These analyses suggest that the Raman enhancement as a function of the ta-C layer thickness could stem mainly from the dramatic change of the localized electromagnetic field of a Ag-based substrate with a dielectric layer.

To confirm this, we have calculated the distance-dependent SERS EF for an individual Ag nanosphere with a coated ta-C film thickness of 10 Å and an uncoated Ag nanosphere that may be considered as a reference for a triangular nanoparticle. Though the shape of nanosphere is different from triangular, the effect of a

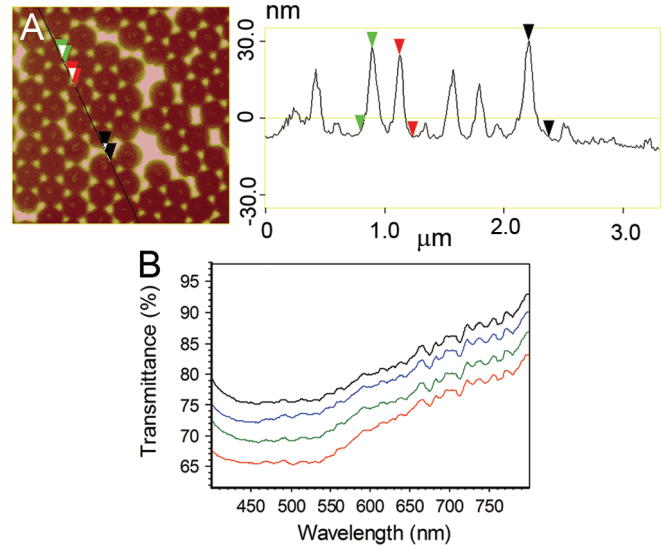

Figure 1. (A) AFM image of the ta-C-coated Ag nanoparticles substrate and (B) transmittance spectra of the Ag nanoparticles array coated with ta-C films having a thickness of 0 Å (black line), 5 Å (blue line), 10 Å (green line), and 20 Å (red line).

dielectric layer modification to the LSP field of a metal nanoparticle surface is very similar. The field enhancement of the coated and uncoated nanospheres was calculated by the Mie theory. In this model, the Ag nanosphere was assumed to have a radius of 50 nm (Figure 4). The dielectric function for Ag was taken from ref 36, and the permittivity of the ta-C films was assumed to be 5.3. In the calculations the field enhancement refers

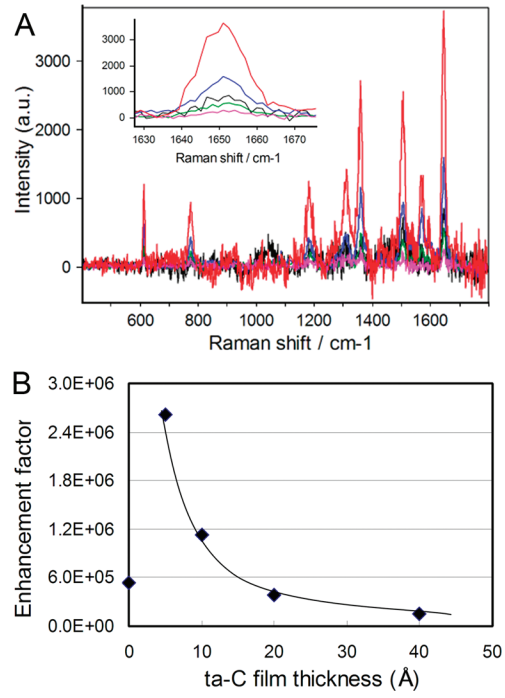

Figure 2. (A) SERS spectra of 10^{-6} M R6G molecules absorbed on the Ag nanoparticle substrates coated with the ta-C layer with a thickness of 0 Å (black line), 5 Å (red line), 10 Å (blue line), 20 Å (green line), and 40 Å (violet line). The inset is a magnification of the 1650 cm^{-1} Raman band. (B) Dependence of the SERS enhancement factor (EF) on the ta-C layer thickness.

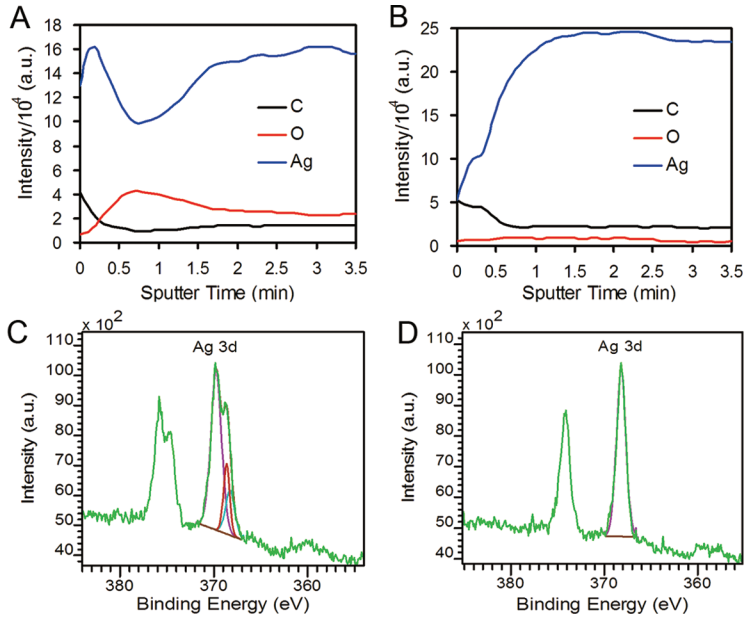

Figure 3. AES depth profile of Ag, O, and C element (A, B) and XPS fine spectra of Ag 3d region (C, D) on the Ag nanoparticle substrates coated with the ta-C films thickness of 5 Å (A, C) and 10 Å (B, D).

to $(E/E_{in})^2$ with E_{in} being the incident field and is evaluated at $\lambda = 403$ nm, which is the LSP resonance of Ag nanosphere. In view of the underlying simplification of the model, it is justified to assume that the SERS EF could be approximated to be $(E/E_{in})^4$. In Figure 4, the SERS enhancement factor $(E/E_{in})^4$ is plotted as a function of the distance from the sphere center ($Z = 0$) and 10 nm ($Z = 10$ nm) and 20 nm ($Z = 20$ nm) from the center of the Ag sphere. It is seen that the field enhancement outside the surface of the Ag sphere coated with ta-C film thickness of 10 Å ($X = 51$ nm for $Z = 0$, $X = 50$ nm for $Z = 10$ nm, and $X = 47$ nm for $Z = 20$ nm), is higher than the surface enhancement for the uncoated Ag sphere ($X = 50$ nm for $Z = 0$, $X = 49$ nm for $Z = 10$ nm, and $X = 46$ nm for $Z = 20$ nm). It is also shown in Figure 4 that the decrease of EF on the Ag sphere coated with a 10 Å ta-C in the directions perpendicular to the interface with distance from the surface is much slower than that on the uncoated Ag nanosphere. These numerical results are in agreement with the experimental findings.

In general, there could be three contributions that lead to an additional enhancement using an ultrathin dielectric layer coated SERS substrate. First, a dielectric layer with a high refractive index can confine light field well. Second, the interference of the scattered light from the inner and outer interfaces partly diminishes the optical field inside the layer. Owing to energy conservation, a relatively larger enhanced field is focused at the outer surface of the dielectric layer. Third, the multiscattering processes of the light scattered back and forth at the two surfaces of the dielectric layers can also contribute to a larger enhancement factor in the cavity.[24] Normally, for a metal nanosphere in a homogeneous dielectric environment, the locally enhanced electric field, which is responsible for the SERS enhancement, is the maximum in the interface and decays exponentially in the directions perpendicular to the interface with distance from the surface.[37] In our case, the local field will decay on the outside surface of the Ag nanoparticle/ta-C layer when the ta-C layer thickness increases from 5 to 40 Å, which is in agreement with experimental findings. When the ta-C layer thickness is increased over 20 Å, the local electric field will be smaller than that of the uncoated substrate.

CONCLUSIONS

We have demonstrated that by being coated with a thin layer of ta-C, a biocompatible and optical transparent dielectric material in the visible region, an Ag nanoparticle-based substrate becomes extremely suitable for SERS. Serving as protective layer, a 10 Å or

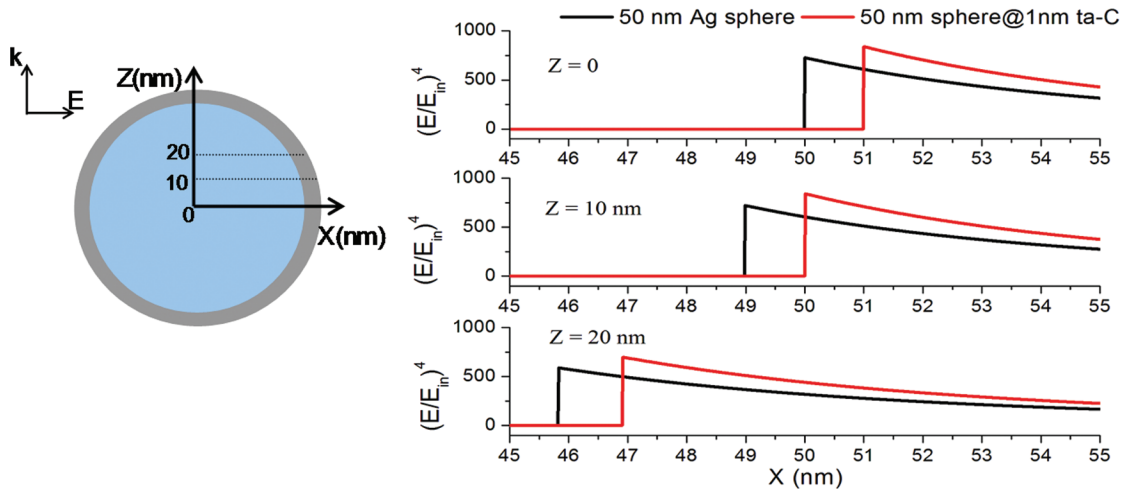

Figure 4. Distance-dependent SERS enhancement factor $(E/E_{in})^4$ calculated for a Ag sphere with a coated ta-C film thickness of 1 nm (red line) and uncoated Ag sphere (black line).

thicker ta-C layer is efficient to protect the oxygen-free Ag in air and prevent Ag ionizing in aqueous solutions. This is important to maintain the chemical stability and biocompatibility for a Ag-based substrate in SERS. In addition, Raman testing shows that increasing the thickness of the coating layer will decrease the Raman enhancement for the coated substrates. Thus, a 10 Å ta-C coating layer is the most suitable to the coated substrates. On the other hand, it is found that a 10 Å ta-C film coated Ag nanoparticle substrate shows a higher enhancement of Raman signals than the uncoated substrate, which is further supported by our numerical simulations. We suggest that biomolecule detections in analytic assays can be easily realized using a 10 Å ta-C-coated Ag-based substrate in SERS, even at the single molecule level.

EXPERIMENTAL SECTION

Silver Nanoparticels Substrates Fabrication. In our experiment, the Ag-based substrates were fabricated using nanosphere lithography as described previously.[29,30] Monodisperse silica nanospheres (400 nm diameter, Duke Scientific) were drop-coated onto a cleaned and base-treated glass substrate and were allowed to dry, forming a hexagonal close-packed monolayer which served as a deposition mask. Ag (99.999% purity) was then sputtered on the top of the nanospheres in a vacuum chamber. Subsequent removal of the nanosphere mask *via* tape stripping left a highly ordered array of relatively uniform triangular silver nanoparticles.

Ta-C Films Deposition. The Ag prepared nanoparticles substrate was further coated with an ultrathin ta-C film using a multifilm deposition system (Shimadzu, MR3, in SAE Magnetics (H.K) Ltd.)) with a combination of a FCVA (filtered cathodic vacuum arc) gun (Nanofilm Technology International, Singapore).[23] The deposition rate monitored by an ellipsometer was ~0.5 Å per second and the film thickness was varied from 5 to 40 Å. Prior to deposition, all the substrates were cleaned by RF-plasma sputtering using Ar ion plasma. The refractive index of the ta-C film was measured to be ~2.3 in the spectrum range from 400 to 1000 nm. In addition, the refractive index of ta-C films almost had no change from 5 to 40 Å. A water contacted angle (WCA) of ~68° of the ta-C film was measured, which showed that the prepared ta-C films are hydrophilic. After films deposition, the roughness had a ~0.5 Å increase due to ion beam sputtering for cleaning before coating.

Characterizations and Raman Testing. The morphology of Ag nanoparticles was explored with a Digital Instrument Nanoscope atomic force microscope (AFM) in tapping mode. For evaluation of the efficiency of the prepared dielectric-coated Ag nanoparticles as a SERS substrate, an aqueous solution of Rhodamine 6G (R6G) 10^{-6} M was used. To allow the molecule adsorption, the prepared substrates were maintained in R6G solution for 24 h, taken out and rinsed thoroughly with ethanol, and finally dried with nitrogen gas. SERS spectra were acquired using a Renishaw Invia Raman microscope system with the laser operating at a wavelength of λ =514 nm with 0.2 mW laser output power, 10 s collection time, and a 50× magnification objective. In addition, Auger electron spectroscopy (AES) was performed on a PHI 680 scanning Auger multiprobe with an incident energy of 5 KV and 10 nA (conditions: 0.5 KV of etching energy and 1 mm^2 etching area; acquiring spectra of Ag, O, and C element every 6 s). X-ray photoelectron spectroscopy (XPS) was also performed on a Shimadzu ESCA 3600 system with an Mg Ka (1253.6 eV) source and the bonding energy (84.0 EV) of Au $4f_{2/7}$ as calibration.

Acknowledgment. The authors gratefully acknowledge SAE Magnetics (H.K) Ltd. for DLC films coating and refractive index measurements. The work was sponsored by the State Key Program for Basic Research of China and NSFC under Grant Nos. 10734010, 50771054, and 10804044. This work was also supported in part by Jiang-Su planned projects for Postdoctoral Research Funds under Grant No. 0901015B.

REFERENCES AND NOTES

1. Nie, S. M.; Emory, S. R. Probing Single Molecules and Single Nanoparticles by Surface-Enhanced Raman Scattering. *Science* **1997**, *275*, 1102–1106.
2. Kneipp, K.; Wang, Y.; Kneipp, H.; Kneipp, H.; Perelman, L. T.; Dasari, R. R.; Feld, M. S. Single Molecule Detection Using Surface-Enhanced Raman Scattering (SERS). *Phys. Rev. Lett.* **1997**, *78*, 1667–1670.
3. Xu, H. X.; Bjerneld, E. J.; Kall, M.; Borjesson, L. Spectroscopy of Single Molecules by Surface Enhanced Raman Scattering. *Phys. Rev. Lett.* **1999**, *83*, 4357–4360.
4. Doering, W. E.; Piotti, M. E.; Natan, M. J.; Freeman, R. G. SERS as a Foundation for Nanoscale, Optically Detected Biological Labels. *Adv. Mater.* **2007**, *19*, 3100–3108.
5. Natan, M. J. Concluding Remarks, Surface Enhanced Raman Scattering. *Faraday Discuss.* **2006**, *132*, 321–328.
6. Feng, J. J.; Gernert, U.; Sezer, M.; Kuhlmann, U.; Murgida, D. H.; David, C.; Richter, M.; Knorr, A.; Hildebrandt, P.; Weidinger, I. M. Novel Au−Ag Hybrid Device for Electrochemical SERR Spectroscopy in a Wide Potential and Spectral Range. *Nano Lett.* **2009**, *9*, 298–303.
7. Jensen, T. R.; Malinsky, M. D.; Haynes, C. L.; Richard, P. Van Duyne. Nanosphere Lithography: Tunable Localized Surface Plasmon Resonance Spectra of Silver Nanoparticles. *J. Phys. Chem. B* **2000**, *104*, 10549–10556.
8. Felidj, N.; Aubard, J.; Levi, G.; Krenn, J. R.; Hohenau, A.; Schider, G.; Leitner, A.; Aussenegg, F. R. Optimized Surface-Enhanced Raman Scattering on Gold Nanoparticle Array. *Appl. Phys. Lett.* **2003**, *82*, 3095–3097.
9. Michaels, A. M.; Jiang, J.; Brus, L. Ag Nanocrystal Junctions as the Site for Surface-Enhanced Raman Scattering of Single Rhodamine 6G Molecules. *J. Phys. Chem. B* **2000**, *104*, 11965–11971.
10. Sztainbuch, I. W. The Effects of Au Aggregate Morphology on Surface-Enhanced Raman Scattering Enhancement. *J. Chem. Phys.* **2006**, *125*, 124707-1–124707-10.
11. Erol, M.; Han, Y.; Stanley, S.; Sukhishvili, S. SERS Not To Be Taken for Granted in the Presence of Oxygen. *J. Am. Chem. Soc.* **2009**, *131*, 7480–7481.
12. Hodak, J. H.; Henglein, A.; Giersig, M.; Hartland, G. V. Laser-Induced Inter-diffusion in Au/Ag Core−Shell Nanoparticles. *J. Phys. Chem. B* **2000**, *104*, 11708–11718.
13. Pande, S.; Ghosh, S. K.; Praharaj, S.; Panigrahi, S.; Basu, S. Synthesis of Normal and Inverted Gold−Silver Core−Shell Architectures in β-Cyclodextrin and Their Applications in SERS. *J. Phys. Chem. C* **2007**, *111*, 10806–10813.
14. Tian, Z. Q.; Ren, B.; Li, J. F.; Yang, Z. L. Expanding Generality of Surface-Enhanced Raman Spectroscopy with Borrowing SERS Activity Strategy. *Chem. Commun.* **2007**, 3514–3534.
15. Kim, K.; Yoon, J. K. Raman Scattering of 4-Aminobenzenethiol Sandwiched between Ag/Au Nanoparticle and Macroscopically Smooth Au Substrate. *J. Phys. Chem. B* **2005**, *109*, 20731–20736.
16. Robertson, J. Diamond-like Amorphous Carbon. *Mater. Sci. Eng. Rep.* **2002**, *37*, 129–281.
17. Robertson, J. Ultrathin Carbon Coatings for Magnetic Storage Technology. *Thin Solid Films* **2001**, *383*, 81–88.
18. Akita, N.; Konishi, Y.; Ogura, S.; Imamura, M.; Hu, Y. H.; Shi, X. Comparison of Deposition Methods for Ultrathin DLC Overcoat Film for MR Head. *Diamond Relat. Mater.* **2001**, *10*, 1017–1023.
19. Liu, F. X.; Wang, Z. L. Thickness Dependence of the Structure of Diamond-like Carbon Films. *Surf. Coat. Technol.* **2009**, *203*, 1829–1832.
20. Chen, J. Y.; Wang, L. P.; Fu, K. Y.; Huang, N.; Leng, Y.; Leng,

Y. X.; Yang, P.; Wang, J.; Wan, G. J.; Chu, P. K.; *et al*. Blood Compatibility and sp^3/sp^2 Contents of Diamond-like Carbon (DLC) Synthesized by Plasma Immersion Ion Implantation-Deposition. *Surf. Coat. Technol.* **2002**, *156*, 289–294.
21. Dearnaley, G.; Arps, H. J. Biomedical Applications of Diamond-like Carbon (DLC) Coatings: A Review. *Surf. Coat. Technol.* **2005**, *200*, 2518–2524.
22. Yokota, T.; Terai, T.; Kobayashi, T.; Iwaki, M. Cell Adhesion to Nitrogen-Doped DLCS Fabricated by Plasma-Based Ion Implantation and Deposition Method. *Nucl. Instrum. Methods Phys. Res., Sect. B* **2006**, *242*, 48–50.
23. Fedel, M.; Motta, A.; Maniglio, D.; Migliaresi, C. Surface Properties and Blood Compatibility of Commercially Available Diamond-like Carbon Coatings for Cardiovascular Devices. *J. Biomed. Mater. Res., Part B: Appl. Biomater.* **2008**, 338–349.
24. Xu, H. X. Theoretical Study of Coated Spherical Metallic Nanoparticles for Single-Molecule Surface-Enhanced Spectroscopy. *Appl. Phys. Lett.* **2004**, *85*, 5980–4982.
25. Pompa, P. P.; Martiradonna, L.; Torre, A. D.; Sala, F. D.; Manna, L.; Vittorio, M. D.; Calabi, F.; Cingolani, R.; Rinaldi, R. Metal-Enhanced Fluorescence of Colloidal Nanocrystals with Nanoscale Control. *Nat. Nanotechnol.* **2006**, *1*, 126–130.
26. Noginov, M. A.; Zhu, G.; Belgrave, A. M.; Bakker, R.; Shalaev, V. M.; Narimanov, E. E.; Stout, S.; Herz, E.; Suteewong, T.; Wiesner, U. Demonstration of Spaser-Based Nanolaser. *Nature* **2009**, *460*, 1110–1112.
27. Jakob, M.; Levanon, H. Charge Distribution Between UV-Irradiated TiO_2 and Gold Nanoparticles: Determination of Shift in the Fermi Level. *Nano Lett.* **2003**, *3*, 353–358.
28. Haes, A. J.; Hall, W. P.; Chang, L.; Klein, W. L.; Richard, P. Van Duyne. A Localized Surface Plasmon Resonance Biosensor: First Steps Toward an Assay for Alzheimer's Disease. *Nano Lett.* **2004**, *4*, 1029–1034.
29. Christy, L. H.; Richard, P. Van Duyne. Nanosphere Lithography: A Versatile Nanofabrication Tool for Studies of Size-Dependent Nanoparticle Optics. *J. Phys. Chem. B* **2001**, *105*, 5599–5611.
30. Zhan, P.; Wang, Z. L.; Dong, H.; Sun, J.; Wu, J.; Wang, H. T.; Zhu, S. N.; Zi, J. The Anomalous Infrared Transmission of Gold Films on Two-Dimensional Colloidal Crystals. *Adv. Mater.* **2006**, *18*, 1612–1616.
31. Baia, M.; Baia, L.; Astilean, S.; Popp, J. Surface-Enhanced Raman Scattering Efficiency of Truncated Tetrahedral Ag Nanoparticle Arrays Mediated by Electromagnetic Coupling. *Appl. Phys. Lett.* **2006**, *88*, 143121–3.
32. Murray, W. A.; Suckling, J. R.; Barnes, W. L. Overlayers on Silver Nanotriangles: Field Confinement and Spectral Position of Localized Surface Plasmon Resonances. *Nano Lett.* **2006**, *6*, 1772–1777.
33. Murray, W. A.; Auguie, B.; Barnes, W. L. Sensitivity of Localized Surface Plasmon Resonances to Bulk and Local Changes in Optical Environment. *J. Phys. Chem. C* **2009**, *113*, 5120–5125.
34. Liu, Y. C.; Yang, K. H.; Hsu, T. C. Improved Surface-Enhanced Raman Scattering Performances on Silver-Silica Nanocomposites. *J. Phys. Chem. C* **2009**, *113*, 8162–8168.
35. Kneipp, K.; Wang, Y.; Dasari, R. R.; Feld, M. S. An Approach to Single Molecule Detection Using Surface-Enhanced Resonance Raman Scattering (SERRS): A Study Using Rhodamine 6G. *Appl. Spectrosc.* **1995**, *49*, 780–784.
36. Johnson, P. B.; Christy, R. W. Optical Constants of the Novel Metals. *Phys. Rev. B* **1972**, *6*, 4370–4379.
37. Barnes, W. L.; Dereux, A.; Ebbesen, T. W. Surface Plasmon Subwavelength Optics. *Nature* **2003**, *424*, 824–830.